



# SERGHEI v2.0: introducing a performance-portable, high-performance, three-dimensional variably saturated subsurface flow solver (SERGHEI-RE)

Zhi Li<sup>1</sup>, Gregor Rickert<sup>2</sup>, Na Zheng<sup>1</sup>, Zhibo Zhang<sup>1</sup>, Ilhan Özgen-Xian<sup>2</sup>, and Daniel Caviedes-Voullième<sup>3,4</sup>

<sup>1</sup>College of Civil Engineering, Tongji University, Shanghai, China

<sup>2</sup>Institute of Geoecology, Technische Universität Braunschweig, Braunschweig, Germany

<sup>3</sup>Simulation and Data Lab Terrestrial Systems, Jülich Supercomputing Centre, Forschungszentrum Jülich, Jülich, Germany

<sup>4</sup>Institute of Bio- and Geosciences Agrosphere (IBG-3), Forschungszentrum Jülich, Jülich, Germany

**Correspondence:** Zhi Li (zli90@tongji.edu.cn)

Received: 16 August 2024 – Discussion started: 5 September 2024

Revised: 2 December 2024 – Accepted: 4 December 2024 – Published: 31 January 2025

**Abstract.** Advances in high-performance parallel computing have significantly enhanced the speed of large-scale hydrological simulations. However, the diversity and rapid evolution of available computational systems and hardware devices limit model flexibility and increase code maintenance efforts. This paper introduces SERGHEI-RE, a three-dimensional, variably saturated subsurface flow simulator within the SERGHEI model framework. SERGHEI-RE adopts the Kokkos-based portable parallelization framework of SERGHEI, which facilitates scalability and ensures performance portability on various computational devices. Moreover, SERGHEI-RE provides options to solve the Richards equation (RE) with iterative or non-iterative numerical schemes, enhancing model flexibility under complex hydrogeological conditions. The solution accuracy of SERGHEI-RE is validated using a series of benchmark tests, ranging from simple infiltration problems to practical hydrological, geotechnical, and agricultural applications. The scalability and performance portability of SERGHEI-RE are demonstrated on a desktop workstation, as well as on multi-CPU and multi-GPU clusters, indicating that SERGHEI-RE is an efficient, scalable, and performance portable tool for large-scale subsurface flow simulations.

## 1 Introduction

In 2022, the Frontier supercomputer with 1.206 exaFLOPS of computing power went online, marking the beginning of the exascale computing era, which will promote previously unfeasible advanced modeling studies in various fields (Chang et al., 2023). Exascale computing will also benefit computational hydrologists who study complex multiscale hydrological processes at catchment to regional scales. Such studies often require the numerical simulation of variably saturated subsurface flow, which can be computationally intensive due to the nonlinear governing equations and the wide ranges of spatial and temporal scales involved (Farthing and Ogden, 2017; Mao et al., 2021; Paniconi and Putti, 2015; Zha et al., 2019).

Most modern physically based integrated hydrological models use the Richardson–Richards equation (Richardson, 1922; Richards, 1931) (hereinafter referred to as Richards equation for historical reasons) to describe variably saturated subsurface flow; see, for example, Paniconi and Putti (2015). Here, a critical challenge is that, due to the nonlinearity of the equation itself and to the required closure relationships for soil-water retention and soil hydraulic conductivity, no numerical scheme achieves accuracy, efficiency, and robustness simultaneously (Farthing and Ogden, 2017). The performance of a numerical scheme is problem dependent, which can be related to the soil properties, the soil moisture conditions, and the boundary conditions. In a comparison study between popular solution schemes, Li et al. (2024) showed

that for some simulation scenarios most numerical schemes achieved satisfactory results. For other scenarios, however, only specific schemes can produce reasonable simulation results. Generally, iterative schemes (such as the modified Picard scheme) adopt a greater time step size ( $\Delta t$ ), but they could fail to converge under certain soil types or soil moisture conditions. Non-iterative schemes, on the contrary, are typically easy to converge, but a smaller  $\Delta t$  is required that increases the computational cost. A more detailed explanation of these two types of numerical schemes will be provided in Sect. 2.2. Additional challenges regarding efficient time stepping, treatment of boundary conditions, and estimation of the interfacial conductivity further complicate the design or selection of numerical Richards solvers (D'Haese et al., 2007; El-Kadi and Ling, 1993; Lai and Ogden, 2015; Paniconi and Putti, 1994; Zha et al., 2016).

Subsurface flow simulations in the hydrological context are often performed over spatial scales that horizontally go from hillslope to the catchment scale and vertically go to hundreds of meters into the subsurface (Condon et al., 2020; Özgen-Xian et al., 2023). The temporal scales of such simulations are often a couple of years to decades. These spatiotemporal scales are usually magnitudes larger than the required resolutions to accurately represent the involved hydrological processes. Although relatively coarse grid resolutions are generally accepted for modeling fully saturated groundwater in the deeper soil layers, in the unsaturated zone grid resolution is often significantly refined below a meter to capture the local flow field (e.g., sharp infiltration fronts). The time step size is reduced accordingly to maintain convergence and stability; see Caviedes-Voullième et al. (2013) and Hou et al. (2022). This results in a heavy computational burden. Some existing models address this issue by assuming one-dimensional (1D) flow in the unsaturated zone, but this assumption leads to biased model predictions when lateral flow is significant (Mao et al., 2021; Shen and Phanikumar, 2010).

Instead of model simplification, high-performance computing (HPC) through massive parallelization provides the computational capabilities to simulate high-resolution, full-dimensional subsurface flow. Richards solvers in most modern hydrological models have parallel computing capabilities, e.g., Amanzi-ATS (Coon et al., 2019), PFLOTRAN (Hammond et al., 2014), ParFlow (Kollet and Maxwell, 2006), Hydrus2D/3D (Šimůnek et al., 2016), and Richards-FOAM (Orgogozo et al., 2014). A foreseeable challenge for many of these models – especially in the exascale era – is the plethora of parallel programming models and their rapid evolution, especially for GPU solutions. Well-established standards, such as OpenMP and MPI, are highly portable across HPC systems. However, GPU programming models (CUDA, HIP) are hardware dependent. In order to allow for models to be deployed on as many HPC systems as possible, maintaining multiple programming models in the source code that target different HPC architectures becomes necessary. While

this results in complex code and increased software maintenance efforts (technical debt), not providing these capabilities will significantly limit the model's applicability in “real-world” use cases (Hokkanen et al., 2021). There are additional challenges when porting software across HPC systems related to supporting robust and general workflows to deal with different software stacks, file systems, schedulers, and so on. We do not address these issues in this paper.

A key challenge that arises when maintaining multiple programming models in the source code is performance portability, i.e., the assurance that the parallel performance and scalability of the code is preserved across different HPC hardware. To the best of our knowledge, despite its importance, performance portability has not yet been the focus of the computational hydrology community. An exception is the ParFlow model that proposed to use an embedded domain-specific language (eDSL) to achieve performance portability, but its performance has not been demonstrated on a wide range of hydrological applications and computational systems (Hokkanen et al., 2021).

The Simulation Environment for Geomorphology, Hydrodynamics, and Ecohydrology in Integrated form (SERGHEI) is an open-source multiphysics modeling framework for environmental, hydrological, and earth system simulations that aims to address the issue of performance portability in computational hydrology. Performance portability is achieved through the Kokkos programming model, which provides flexibility when switching between different computational platforms, by abstracting hardware-dependent code and thus enhancing development productivity and facilitating maintenance (Trott et al., 2022). This means that the same code can be compiled to allow for CPU parallelization (e.g., OpenMP) and GPU parallelization (e.g., CUDA); thus, there is no need to maintain different programming models in the SERGHEI code base. In this paper, we introduce SERGHEI-RE, the Richards-equation-based variably saturated subsurface flow module of SERGHEI.

In the following, the accuracy, robustness, scalability, and portability of the SERGHEI-RE module is demonstrated through a series of numerical tests ranging from simple idealized problems to large-scale realistic problems (Sects. 4 and 5). SERGHEI-RE is designed both as a standalone variably saturated subsurface flow model and as part of the integrated surface–subsurface flow simulator under the SERGHEI framework. In this paper, we focus on demonstrating its performance as a Richards equation solver only. Moreover, we focus on the performance portability of the SERGHEI-RE solver, and we purposely do not delve into the workflows required to build and run the software, although minimal support for this is included in the software release.

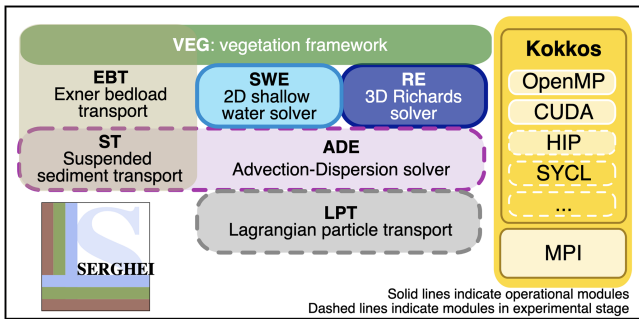


**Figure 1.** An overview of the SERGHEI model components modified from Caviedes-Voullième et al. (2023). The solid lines indicate operational modules. The dashed lines indicate modules in the experimental stage. Modules without lines are still in the conceptual stage.

## 2 Model description

### 2.1 An overview of SERGHEI

SERGHEI features a modular design that allows for different modules that represent different ecohydrological/hydraulic processes to be dynamically coupled at compile time. The modular architecture of SERGHEI and its existing modules is depicted in Fig. 1. At the time of writing, different modules are at different stages of development. The most mature module of SERGHEI is its fully dynamic surface hydrology solver based on the shallow water equations, released as SERGHEI-SWE in Caviedes-Voullième et al. (2023). The subsurface flow solver SERGHEI-RE is introduced in the following. The coupling of SERGHEI-SWE and SERGHEI-RE to obtain an integrated hydrological solver is currently functional but requires further verification of correctness, numerical accuracy, and performance portability. A general advection–dispersion equation solver (SERGHEI-ADE) is functional and serves as a base for the suspended sediment transport module (SERGHEI-ST). Lagrangian particle transport (SERGHEI-LPT) and an Exner-equation-based bedload transport module (SERGHEI-EBT) are under development. Finally, the infrastructure to couple SERGHEI with ecosystem models (SERGHEI-ECO) is in early stages of development.

Within this framework, SERGHEI-RE plays a key role in the redistribution of water that drives the other processes discussed above. The performance of this module is thus critical for the entire modeling framework. SERGHEI-RE is equipped with two key features that address these performance expectations: (i) SERGHEI-RE allows the user to choose between an iterative and a non-iterative numerical scheme for solving the Richards equation, which enables efficient time integration on HPC systems under various hydrogeological conditions (Sect. 2), and (ii) SERGHEI-RE inherits the Kokkos-based code structure of SERGHEI-SWE, which helps to achieve performance portability on a variety

of computational backends (Sect. 3). Both features aim at enhancing the adaptivity and flexibility of SERGHEI-RE in handling various simulation scenarios and HPC systems.

### 2.2 Numerical methods

In this section, we describe the numerical schemes applied to solve the Richards equation. The generalized (i.e., considering the compressibility effect when the soil is fully saturated) three-dimensional (3D) Richards equation is presented in Eq. (1) in its mixed form, where  $S_s [L^{-1}]$  is the specific storage;  $h [L]$  is pressure head;  $\theta [-]$  is water content;  $\phi [-]$  is porosity; and  $\mathbf{q} [L T^{-1}]$  is groundwater flux, which is calculated through a generalized Darcy’s law (Eq. 2).  $\mathbf{K} [L T^{-1}]$  is the hydraulic conductivity,  $z [L]$  is elevation, and  $S(x, y, z, t) [T^{-1}]$  represents the source/sink terms.

$$\frac{S_s \theta}{\phi} \frac{\partial h}{\partial t} + \frac{\partial \theta}{\partial t} - \nabla \cdot \mathbf{q} = S(x, y, z, t), \quad (1)$$

$$\mathbf{q} = \mathbf{K} \nabla (h - z). \quad (2)$$

The popular Mualem–van Genuchten (VG) model (Eqs. 3–5) is used for describing the soil-water retention characteristics (Mualem, 1976; van Genuchten, 1980):

$$s(h) = \left(1 + |\alpha h|^{\tilde{n}}\right)^{-m}, \quad (3)$$

$$\theta(h) = \theta_r + (\phi - \theta_r) s(h), \quad (4)$$

$$K(h) = K_s s(h)^{\frac{1}{2}} \left[1 - \left(1 - s(h)^{\frac{1}{m}}\right)^m\right]^2, \quad (5)$$

where  $s [-]$  is water saturation,  $K_s [L T^{-1}]$  is saturated hydraulic conductivity,  $\theta_r [-]$  is residual water content,  $\alpha [L^{-1}]$  and  $\tilde{n} [-]$  are the soil parameters, and  $m = 1 - 1/\tilde{n}$ . It has been generally acknowledged that  $\alpha$  is related to the air entry value and that  $\tilde{n}$  reflects the particle size distribution (Vogel, 2001; Zhang et al., 2021), but different opinions also exist (van Lier and Pinheiro, 2018).

SERGHEI-RE provides two numerical schemes to solve Eqs. (1)–(5). The default option is the predictor–corrector (PC) scheme proposed by Kirkland et al. (1992). An alternative option is the modified Picard (MP) scheme proposed by Celia et al. (1990). The MP scheme has been widely adopted in popular Richards solvers (Šimůnek et al., 2013), which falls, more generally, under the umbrella of fully implicit solvers which may also use other linearization strategies such as Newton schemes (Kuffour et al., 2020). The MP is an iterative scheme that first solves the linearized Richards equation in its head form as

$$C_h \frac{\partial h}{\partial t} - \nabla \cdot \mathbf{q} = S(x, y, z, t), \quad (6)$$

where  $C(h) = \partial \theta / \partial h$ . Then, the linearization error is corrected iteratively with the correction derived from truncated Taylor series. The main drawback of the MP scheme is that convergence of the linearization iterations is not guaranteed.

Specifically, cases using the modified Picard iteration struggle to converge if abrupt changes in soil moisture occur or when Neumann-type boundary conditions are enforced (Zha et al., 2017).

The PC scheme, on the other hand, corrects the linearization error with an explicit corrector, which avoids iterating and guarantees convergence. The drawback of the PC scheme is that the corrector typically requires smaller time step  $\Delta t$  (in comparison to the fully implicit MP scheme), which could potentially increase the computational cost. Moreover, the PC scheme does not strictly (globally) conserve mass (Lai and Ogden, 2015), although Li et al. (2021) found that the amount of mass lost is often negligible. More detailed descriptions of the PC and MP schemes, as well as a comparison between the two schemes, are available in Li et al. (2021, 2024). It should be noted that using relatively small  $\Delta t$  in the PC scheme is not necessarily unacceptable as SERGHEI-RE will be coupled with the SERGHEI-SWE solver in the future. The  $\Delta t$  of the SWE solver is restricted by the Courant–Friedrichs–Lewy (CFL) condition for stability. If the Richards solver uses very large  $\Delta t$  (i.e., the surface and the subsurface modules are asynchronous), the error on the modeled surface–subsurface exchange flux could be non-negligible for rapidly varying surface flow (Li et al., 2023). Thus, to prepare for model coupling and to acknowledge that no numerical scheme is optimal for the Richards equation under all circumstances, both PC and MP schemes are implemented to provide flexibility for SERGHEI-RE to fit into various simulation conditions and requirements.

Like many existing Richards solvers (e.g., D’Haese et al., 2007; Zha et al., 2019), SERGHEI-RE uses variable  $\Delta t$  to improve computational efficiency. For the PC scheme implemented in SERGHEI-RE,  $\Delta t$  is adjusted based on the maximum change of water content in the previous step. If the maximum change of water content within a time step ( $\Delta\theta_{\max}$ ) is greater than an upper limit,  $\Theta_{\max}$ ,  $\Delta t$  is reduced. If  $\Delta\theta_{\max} < \Theta_{\min}$ ,  $\Delta t$  is increased.  $\Theta_{\max}$  and  $\Theta_{\min}$  are user-defined thresholds. For the MP scheme,  $\Delta t$  is adjusted based on the number of linearization iterations, similar to the solution in Hydrus (Šimůnek et al., 2013). If the number of linearization iterations required for convergence ( $N_{\text{iter}}$ ) is greater than an upper limit,  $N_{\text{iterMax}}$ ,  $\Delta t$  is reduced. If  $N_{\text{iter}} < N_{\text{iterMin}}$ ,  $\Delta t$  is increased.  $N_{\text{iterMax}}$  and  $N_{\text{iterMin}}$  are user-defined thresholds. Acknowledging that both time stepping schemes are somewhat heuristic, an upper limit,  $\Delta t_{\max}$ , is defined as a user input parameter to avoid unwanted large  $\Delta t$  during the simulation. A detailed mathematical description of the time stepping strategies can be found in Li et al. (2024).

### 2.3 User configuration

SERGHEI-RE provides various options for users to control the simulation. These options can be categorized as domain characteristics and flow characteristics.

The subsurface domain is defined using a digital elevation model (DEM) that describes the land surface topography and a height value that describes the thickness of the subsurface domain in the vertical direction. SERGHEI-RE uses structured Cartesian grids with uniform resolutions in the  $x$  and  $y$  directions, which matches the resolution of the DEM input file. In the vertical ( $z$ ) direction, Richards solvers often require extremely small grid resolutions ( $\Delta z$ ) near the ground surface to resolve the infiltration front. To enhance computational efficiency, a variable vertical resolution is allowed in SERGHEI-RE, where  $\Delta z$  gradually increases from top to bottom. The  $\Delta z$  of the  $k$ th layer from the top (i.e., the land surface) is calculated via

$$\Delta z_k = \Delta z_{\text{base}} \beta^k, \quad (7)$$

where  $\Delta z_{\text{base}}$  is the user-provided grid size of the topmost layer, and  $\beta \geq 1$  is the ratio of grid size increment.

SERGHEI-RE enables a terrain-following mesh to resolve topographic variations in the real world. When complex topography exists, the Darcy fluxes (Eq. 2) in the  $x$  and  $y$  directions are modified correspondingly to conform to the terrain slope. The modified Darcy’s law to calculate the horizontal fluxes considering the terrain slope reads as (Maxwell, 2013)

$$\mathbf{q} = \mathbf{K} [\cos \omega \nabla (h - z) + \sin \omega]. \quad (8)$$

where  $\omega$  is the angle between the connection of two cell centers and the horizontal axis. Note that (i) when applying Eq. (8) the bottom boundary of the subsurface domain follows the terrain slope, too, and that (ii) the vertical flux is unchanged when terrain slope exists.

The subsurface domain can be heterogeneous. To model a heterogeneous system, the user should provide  $N$  groups of soil parameters (each group includes the saturated hydraulic conductivity, saturated/residual water content, and  $\alpha$  and  $\tilde{n}$  parameters of the VG model) and a soil type index (ranging from 0 to  $N - 1$ ) for each grid cell. In this way, the heterogeneous subsurface domain can be described on a cell-by-cell basis. Figure 2 shows an example of two soil types indexed as 0 and 1. Currently, SERGHEI-RE does not yet support multi-porosity subsurface domains.

The flow characteristics consist of the initial and boundary conditions and the source/sink terms. SERGHEI-RE accepts various types of initial and boundary conditions. The user can specify the spatially distributed initial pressure head and water content, or they can specify the initial elevation of the groundwater table. For the latter case, the initial pressure head will be calculated following the hydrostatic pressure distribution. Both Dirichlet (constant, space-varying, or time-varying pressure head) and Neumann (constant, space-varying, or time-varying flux) boundary conditions are accepted for all the boundaries. For lateral boundaries, water table elevation is also an accepted form of boundary condition, which is then converted to hydrostatic pressure distribution along the boundary. For the top boundary, a special interface

is implemented to allow for reading variables from the SWE solver, which is reserved for surface–subsurface model coupling in the future. The boundary conditions can be applied to the entire topological boundary surface or only to a certain subset of it. Similar to SERGHEI-SWE, this is achieved by defining a “polyhedron” that delineates a range in space in which boundary conditions are enforced. The idea of a polyhedron is also used for defining internal source/sink terms. For example, users can delineate a cuboid in the 3D subsurface domain, within which a flux source (e.g., irrigation) or sink (e.g., root water uptake) term is applied. Similar to the boundary conditions, the source/sink data can be constant, space-varying, or time-varying.

### 3 HPC implementation

Similar to SERGHEI-SWE, the SERGHEI-RE model features both shared memory and distributed memory parallelism on both multicore CPUs and GPUs (Fig. 1). The performance-portable shared memory parallelism is implemented under the Kokkos framework, which has been described in detail in Caviedes-Voullième et al. (2023). The distributed memory parallelism is implemented through MPI. The 3D subsurface domain is partitioned with a 2D domain decomposition into the  $x$  and  $y$  directions, and the subsurface state variables (e.g.,  $h$ ,  $\theta$ ) along the boundaries are exchanged between adjacent subdomains. The key difference between the data exchange in SERGHEI-RE and SERGHEI-SWE is that in SERGHEI-RE the internal subdomain boundaries (i.e., the boundaries of subdomains on which data exchange occurs) are planar rather than linear. As a result, the MPI send and receive functions have been rewritten to manipulate the planar data. To facilitate the coupled surface–subsurface model development in the future, the vertical coordinate of the subsurface domain is not partitioned into subdomains. This ensures that surface hydrodynamics are modeled in all subdomains, which achieves better load balancing (Fig. 2).

For both the PC and MP schemes, SERGHEI-RE requires a linear solver to solve for the pressure head from the linearized Richards equation (Li et al., 2024). To complete this task, the preconditioned conjugate gradient (PCG) solver provided in Kokkos Kernels is implemented in SERGHEI-RE. Kokkos Kernels is a linear algebra library under the Kokkos ecosystem. The main advantage of using Kokkos Kernels is that it is compatible with the Kokkos framework in terms of data structures, computing spaces, and overall performance portability. This is demonstrated through the scaling test in Sect. 5. Finally, it should be pointed out that when the domain is decomposed each subdomain forms its own linear system. Data transferred across subdomains are inevitably lagged by one time step, but this has a negligible influence on solution accuracy for the numerical tests performed in this study.

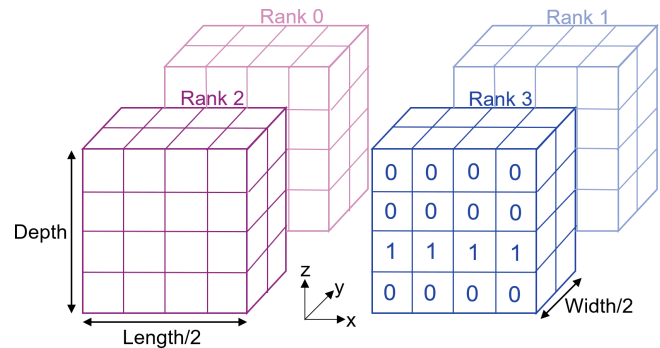


**Figure 2.** An example of the SERGHEI-RE domain decomposition with two subdomains in the  $x$  and  $y$  directions. The  $z$  direction is not decomposed. In Rank 3, the cell-by-cell soil indices are labeled, which consist of two types of soil that form three layers.

### 4 Model verification

This section reports the benchmark tests for verifying SERGHEI-RE. Table 1 summarizes the six test problems used herein, including the domain dimension, the types of initial/boundary condition, soil heterogeneity, and terrain slope. In addition to traditional hydrological tests, we also include tests in the field of geotechnical engineering (Sect. 4.5) and agriculture (Sect. 4.6) to demonstrate the broad range of potential applicability of SERGHEI-RE. Results of the first two test problems are generated on an Intel Core i9-9880H processor (eight cores, 16 threads, 2.3 GHz). The other four tests are completed on an Nvidia RTX A5000 GPU (24 GB memory, 768 GB s<sup>-1</sup> bandwidth).

#### 4.1 1D infiltration

The first test is a 1D infiltration problem from Warrick et al. (1985). A fixed pressure head of 0 m is applied to the top of a soil column. The column is nearly dry, with a uniform water content of 0.03 as the initial condition. This problem has been widely used to validate Richards solvers, because analytical solutions have been derived (Caviedes-Voullième et al., 2013; Lai and Ogden, 2015; Li et al., 2021; Phoon et al., 2007). A total of eight simulation scenarios are established, with two different numerical schemes (PC, MP), two different  $\Delta t_{\max}$  values (0.4 s, 10 s), and three different grid resolutions ( $\Delta z = 0.01$  m,  $\Delta z = 0.02$  m, and a variable  $\Delta z$  between 0.01 m (top) and 0.03 m (bottom)). The three grid resolutions result in 100, 50, and 56 grid cells, respectively, along the soil column.

Figure 3 shows the water content profiles modeled with SERGHEI-RE (all with  $\Delta t_{\max} = 0.4$  s), as well as the analytical solutions at the corresponding times. It can be seen from Fig. 3a that with  $\Delta z = 0.01$  m both the PC and MP schemes achieve good agreements with the analytical solution. As  $\Delta z$  increases, the infiltration speed is overestimated. Clearly, the solution accuracy is sensitive to the grid resolution (Li et al.,

**Table 1.** A summary of model verification tests. D and N refer to Dirichlet (pressure of water table) and Neumann (flux) boundary conditions (BCs), respectively. Top, bottom, and sides indicate which boundary the BC is applied to. S refers to a source or sink. The Soil column indicates whether the soil texture is homogeneous (H) or heterogeneous (NH). The Slope column indicates the presence of a topographic slope.

Section	Dimension	Type of IC	Type of BC	Soil	Slope	Source
4.1	1D	Dry	D (top)	H	–	Warrick et al. (1985)
4.2	1D	Saturated	D (bottom)	H	–	Abeele (1984)
4.3	2D	Dry	N (top)	NH	No	Kirkland et al. (1992)
4.4	2D	Pressure	D (sides), N (top)	H	Yes	Morway et al. (2013)
4.5	2D	Water table	D (top, bottom)	H	Yes	Chávez-Negrete et al. (2018)
4.6	2D	Water Content	N (top, bottom) + S	NH	No	He et al. (2018)

**Table 2.** A summary of the eight simulation scenarios of the 1D infiltration problem. The numerical scheme,  $\Delta z$ ,  $\Delta t_{\max}$ , RMSE, and the simulation time are listed.

Numerical scheme	$\Delta z$ [m]	Number of cells	$\Delta t_{\max}$ [s]	RMSE [cm]	Runtime [s]
PC	0.01	100	0.4	0.5823	161.6
MP	0.01	100	0.4	0.5811	175.8
PC	0.02	50	0.4	1.6483	98.4
MP	0.02	50	0.4	1.6484	108.6
PC	Variable	56	0.4	0.9339	104.5
MP	Variable	56	0.4	0.9329	115.7
PC	0.01	100	10	0.7308	10.9
MP	0.01	100	10	0.5987	35.1

2021). A closer look at the infiltration fronts (Fig. 3b) reveals negligible difference between the PC and MP schemes.

More insights are obtained from Table 2, where the root-mean-square errors (RMSEs, in terms of the depth difference between the modeled infiltration fronts and the analytical solution) and the computational cost are listed. Compared with a uniform  $\Delta z$  of 0.02 m, using variable  $\Delta z$  results in approximately 40 % lower RMSE, with only about 7 % increased computational cost. With the same  $\Delta t_{\max}$ , the MP scheme is computationally more expensive than the PC scheme, as it is iterative. However, when  $\Delta t_{\max}$  is set to 10 s, the RMSE of the MP scheme remains low, but the RMSE of the PC scheme increases by 25 %. This indicates that the error of the PC scheme is more sensitive to  $\Delta t_{\max}$ , as the corrector step is fully explicit (Li et al., 2021, 2024). As a result, the MP scheme with  $\Delta t_{\max} = 10$  s is much faster than the PC scheme with  $\Delta t_{\max} = 0.4$  s, despite their comparable RMSEs.

## 4.2 1D drainage

The second test is based on a free drainage experiment by Abeele (1984), which has been previously used for model verification (Caviedes-Voullième et al., 2013; Forsyth et al., 1995; Lai and Ogden, 2015). The computational domain is a homogeneous and initially fully saturated 1D soil column. The bottom of the column is open with a fixed pressure equal

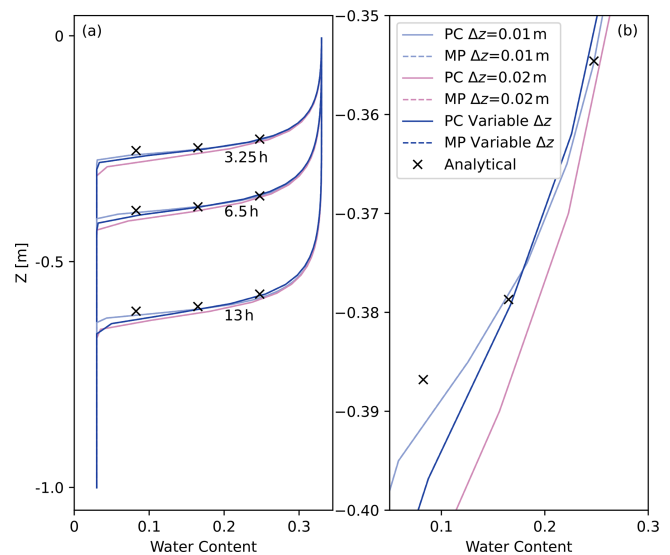


**Figure 3.** SERGHEI-RE simulation results (water content profiles) of Warrick's problem against the analytical solution with different choices of  $\Delta z$ . Panel (a) shows the water content profiles over the entire column, and panel (b) shows a zoomed-in view to examine the profiles in detail.

to atmospheric pressure ( $h = 0$  m). The simulation period is set to 100 d, with  $\Delta z = 0.06$  m and  $\Delta t_{\max} = 1$  d for both the PC and MP schemes. The modeled water content profiles can be found in Fig. 4. SERGHEI-RE generally reaches good agreements with the experimental results, with slight underestimation of the water content on day 100. The PC and MP schemes exhibit negligible difference on this test problem, but the MP scheme requires almost 3 times the computational cost (3.83 s versus 1.33 s).

## 4.3 2D infiltration with layered soil

The third test problem simulates infiltration into layered soil, which has been used for model verification in Bassetto et al. (2022), Kirkland et al. (1992) and Forsyth et al. (1995). The model domain (Fig. 5) is 2D rectangular and consists of two types of soils. Initially, the domain is nearly dry with a uni-

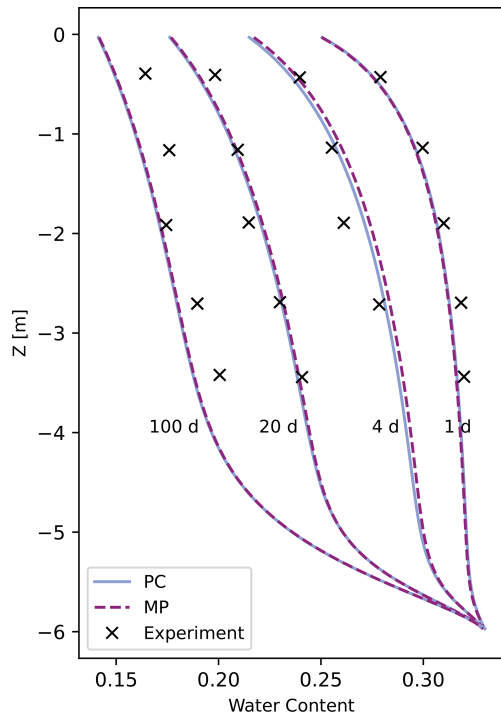


**Figure 4.** SERGHEI-RE simulation results (water content profile) of the drainage problem against the experimental data. The simulations use  $\Delta z = 0.06$  m and  $\Delta t_{\max} = 1$  d.

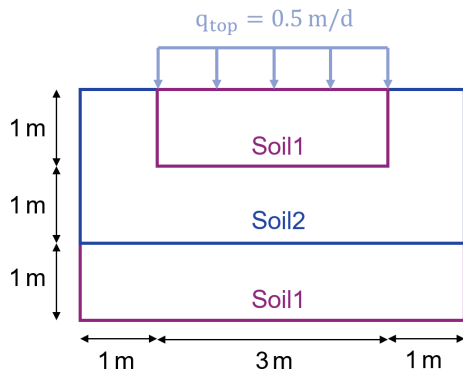


**Figure 5.** Sketch of the model domain for the heterogeneous infiltration problem.

form pressure head of  $-400$  m. A constant infiltration flux is applied to the middle section of the top layer. Since Soil2 has lower permeability than Soil1, as the wetting front infiltrates downward, water will accumulate near the interface between the two soil layers. For this test problem, the MP scheme shows a slow convergence rate. Thus, only the PC scheme is used (with  $\Delta z = 0.1$  m and  $\Delta t_{\max} = 10$  s) to generate results for model verification. As can be seen from Fig. 6, a saturated zone characterized by a positive pressure head is formed at the soil interface as a result of the permeability change. This trend is well captured with SERGHEI-RE.

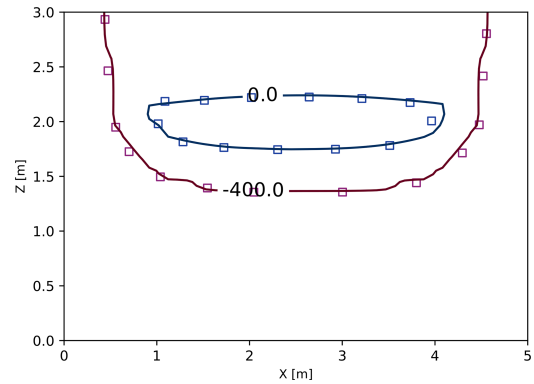


**Figure 6.** The pressure head contours modeled with SERGHEI-RE (solid lines, with PC scheme) and the reference solution (square markers, which is the numerical solution reported in Kirkland et al., 1992) for the 2D infiltration problem at the end of the simulation (1 d). The numbers on the contours are the pressure head values in meters.

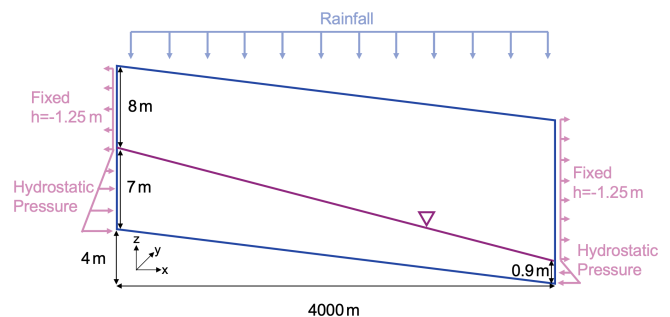


**Figure 7.** The dimension of the model domain and the boundary conditions for the 2D infiltration problem with open lateral boundaries.

#### 4.4 2D infiltration with open lateral boundaries

The fourth problem models rainfall onto an inclined plane with open lateral boundaries (Beegum et al., 2018; Brandhorst et al., 2021; Morway et al., 2013). An illustration of the problem setup is shown in Fig. 7. The water table depth is fixed at 8 and 14.1 m on the left and right boundaries, respectively. Initially, hydrostatic pressure distribution is applied below the water table, and a constant pressure head is enforced above the water table. Rainfall with variable intensity is applied to the top boundary (Table 3). The original problem is 3D. However, since all the grid layers in the  $y$  direction are identical, for model verification purposes a 2D  $x$ – $z$  simulation is sufficient. The 3D version of this test problem is used for the scaling tests described in Sect. 5.

Four simulation scenarios are established for this test case: uniform grid resolution ( $\Delta z = 0.25$  m) with the PC and MP schemes and variable grid resolution ( $\Delta z_{\text{base}} = 0.1$  m,  $\beta = 1.05$ ) with the PC and MP schemes. The uniform and variable resolution scenarios have 60 and 44 grid cells in the ver-

**Table 3.** Monthly variable rainfall intensity used for the 2D infiltration (with lateral flow) test problem. The data shown are for 1 year. It is assumed that each year in the simulation has the same rainfall intensity.

Month	1	2	3	4	5	6
Rainfall [mm h <sup>-1</sup> ]	0.017	0.017	0.042	0.071	0.1	0.079
Month	7	8	9	10	11	12
Rainfall [mm h <sup>-1</sup> ]	0.108	0.088	0.054	0.046	0.025	0.017

**Table 4.** A summary of the four simulation scenarios of the 2D infiltration (with lateral flow) problem. The numerical scheme,  $\Delta z$ , number of cells, and the simulation time are listed.

Numerical scheme	$\Delta z$ [m]	Number of cells	Runtime [min]
PC	0.25	2400	22.45
MP	0.25	2400	38.65
PC	0.1–0.81	1760	13.34
MP	0.1–0.81	1760	25.49

tical direction, respectively. All simulations are performed for 5 years with  $\Delta t_{\max} = 3600$  s. It can be seen from Table 4 that by applying a variable grid resolution the total wall-clock simulation time reduces by 41 % and 34 % for the PC and MP schemes, respectively. With the same  $\Delta t_{\max}$ , the MP scheme is more expensive than the PC scheme. These trends are consistent with those reported in Sect. 4.1 and 4.2.

When rainfall penetrates the top boundary, driven by the horizontal pressure gradient, the infiltrated water will exit the domain through its lateral boundaries. This results in a concave water table. Furthermore, since the rainfall rate varies monthly, the water table elevation fluctuates in time. Figure 8a shows the temporal variation of the water table elevation in the center of the domain, and Fig. 8b shows the water table elevation at the end of the 5-year simulation. It can be seen that all SERGHEI-RE scenarios have good agreements with Hydrus2D, which is used as the reference solution herein. Differences between SERGHEI-RE scenarios are negligible for this test problem.

#### 4.5 2D infiltration into a road embankment

The fifth problem models water infiltration into a 2D partially paved road embankment (Fig. 9). In the original problem, the bottom of the embankment is flat with a constant pressure head of 0 m (Chávez-Negrete et al., 2018). For SERGHEI-RE, however, the terrain-following mesh requires an extended bottom section, resulting in an inclined bottom boundary. To preserve the original water table elevation, a hydrostatic pressure head (calculated from the original water table elevation) is enforced along the inclined bottom boundary. A thin layer of water ( $h = 0$  m) is applied to the open top boundary. The simulation is performed with the PC scheme

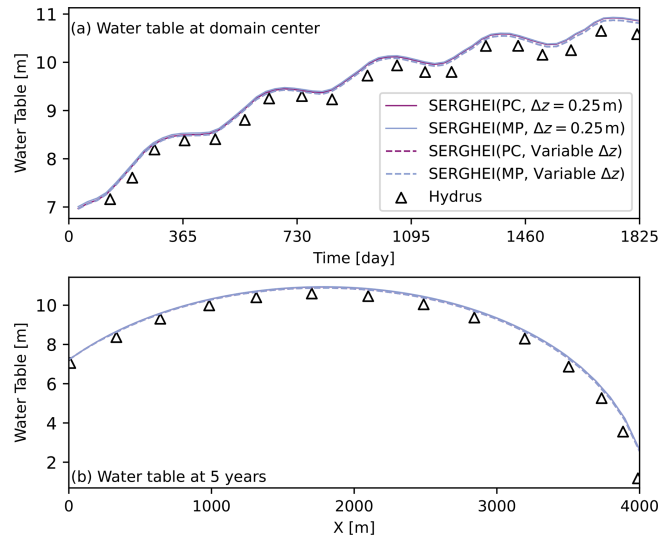


**Figure 8.** SERGHEI-RE simulation results (water table elevation) of the infiltration problem against the Hydrus results.

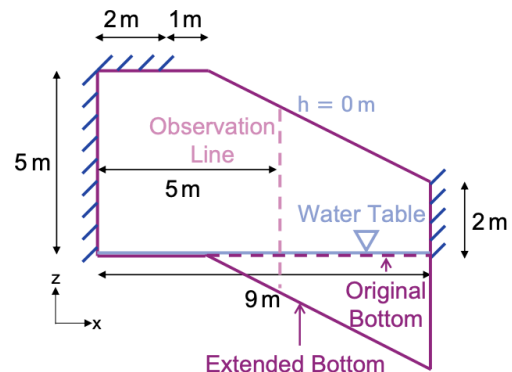


**Figure 9.** Sketch of the model domain and the boundary conditions for the road embankment problem. Dashed lines indicate the required extension due to the terrain-following mesh.

only. The MP scheme is difficult to converge for this test problem.

Figure 10 shows a comparison between the pressure profiles at the observation line (Fig. 9) modeled with SERGHEI-RE and with the generalized finite difference method (GFDM) of Chávez-Negrete et al. (2018). The two results achieve good agreement up to day 1. At 1.5 d, SERGHEI-



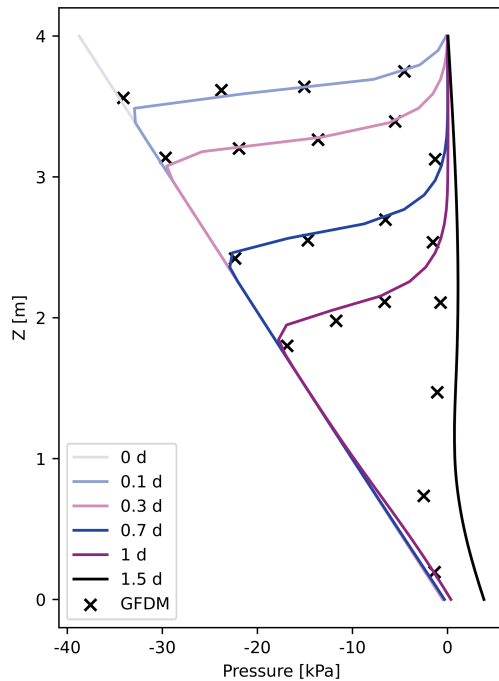


**Figure 10.** SERGHEI-RE simulation results of the infiltration problem against the GFDM results.

RE slightly overestimates the bottom pressure compared to GFDM. This is due to the reason that for the SERGHEI-RE domain the pressure boundary condition is enforced along the inclined bottom not the location of the water table. Thus, during the simulation, the actual water table might slightly deviate from  $z = 0$  m.

#### 4.6 2D crop irrigation

The sixth problem models soil-water dynamics in a real agricultural field. Prior field measurements and numerical simulations at this site are documented in He et al. (2018). The model domain is a 2D vertical transect of the crop field with dimensions, soil layers, and boundary conditions illustrated in Fig. 11a. Note that the model domain built herein is half of the original domain, because the original domain is fully symmetric. The ground surface is partially covered with film mulch, below which drip irrigation is applied. The side boundaries are impermeable, and the bottom boundary is free drainage. The rainfall, evaporation, irrigation, and transpiration rates applied are shown in Fig. 11b and c for years 2014 and 2015, respectively. These data are all provided in He et al. (2018). The rainfall and irrigation data were sampled in the field, whereas the evaporation and transpiration data were simulated. In 2015, the simulation error of soil evaporation increased, shown as the nearly zero evaporation flux after day 50 (Fig. 11c). However, for this test problem, soil evaporation is relatively insignificant compared to other fluxes, and it has a minor influence on soil moisture dynam-

ics. The grid resolutions are  $\Delta x = 0.01$  m and  $\Delta z = 0.01$  m. The maximum  $\Delta t$  is set to 60 s for both the PC and MP schemes tested.

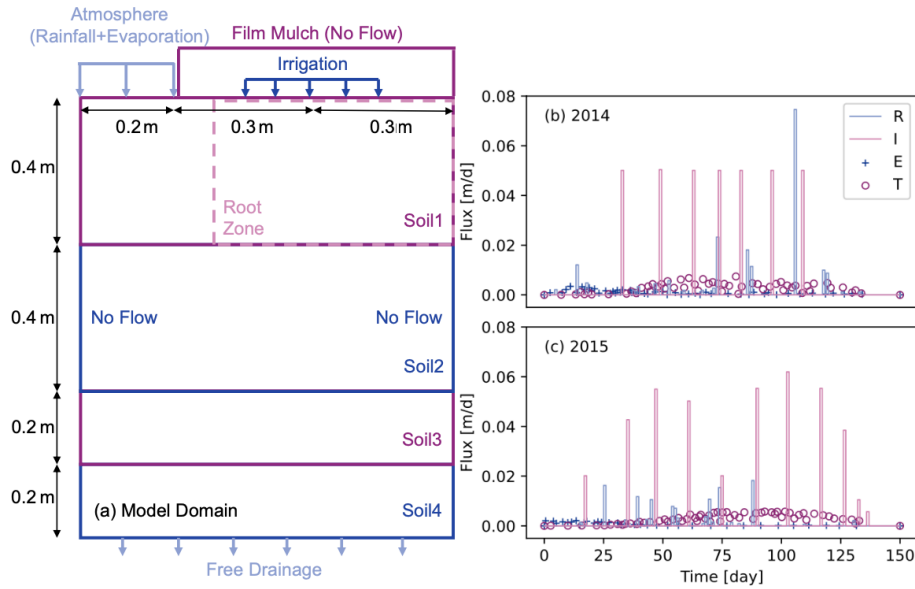
It should be noted that SERGHEI-RE is not particularly designed for agricultural applications. For the time being, SERGHEI-RE does not consider spatially variable and pressure dependent root water uptake, which is different from the treatment in most agricultural hydrologic models (including He et al., 2018). To reproduce the field measurements and numerical modeling results of He et al. (2018), the transpiration rate is treated as a sink term that is uniformly applied to the root zone, whose dimension is used to calibrate SERGHEI-RE. The final width and depth of the root zone are set to be 0.5 and 0.4 m, respectively. Although these features of the problem cannot be fully represented in SERGHEI-RE, this problem is interesting for its multiple boundary fluxes (both inflow and outflow) as well as internal source/sink terms. It is therefore useful to test and validate such features in SERGHEI-RE.

Figure 12 shows the evolution of water content at 0.2 and 0.6 m beneath the irrigation emitter. For years 2014 and 2015, the agreement between SERGHEI-RE and Hydrus2D is reasonably good. The irrigation events, which are implied by the rising water content, are well captured by SERGHEI-RE. The PC and MP schemes produce indistinguishable results for this test problem.

The computational domain consists of four soil layers, four types of boundary conditions (rainfall, evaporation, irrigation, and free drainage), and one internal sink term (root water uptake), making it a challenging test case from a modeling perspective. Figure 12 demonstrates the capability of SERGHEI-RE in simulating soil-water dynamics under complex field conditions. Model discrepancies can be attributed to (i) the uniform root water uptake rate used in SERGHEI-RE and (ii) the possible error in the input data. For example, the first irrigation event in 2015, as evidenced by the rising water content modeled with Hydrus2D (Fig. 12c), is not documented in the irrigation data (He et al., 2018). This might directly lead to the underestimation of water content in the first 40 d of Fig. 12c and d.

## 5 Performance and scaling

An important feature of the SERGHEI-RE model is scalability and performance portability. SERGHEI-RE is designed both for simple idealized simulations on personal laptops and desktops and for large-scale realistic simulations on HPC platforms. To demonstrate the scalability and performance portability of SERGHEI-RE, the rainfall infiltration problem (Sect. 4.4) is extended to 3D with finer grid resolutions ( $\Delta x$ ,  $\Delta y = 5$  m,  $\Delta z = 0.1$  m). By adjusting the width of the computational domain in the  $y$  direction, rainfall infiltration simulations with different numbers of grid cells can be created – 120 000 cells for each additional row in the  $y$  direction.



**Figure 11.** (a) The dimension of the model domain and the boundary conditions for the crop irrigation problem; (b) the rainfall ( $R$ ), irrigation ( $I$ ), soil evaporation ( $E$ ), and root water uptake (transpiration,  $T$ ) rates during the study period in 2014; (c)  $R$ ,  $I$ ,  $E$ , and  $T$  during the study period in 2015.

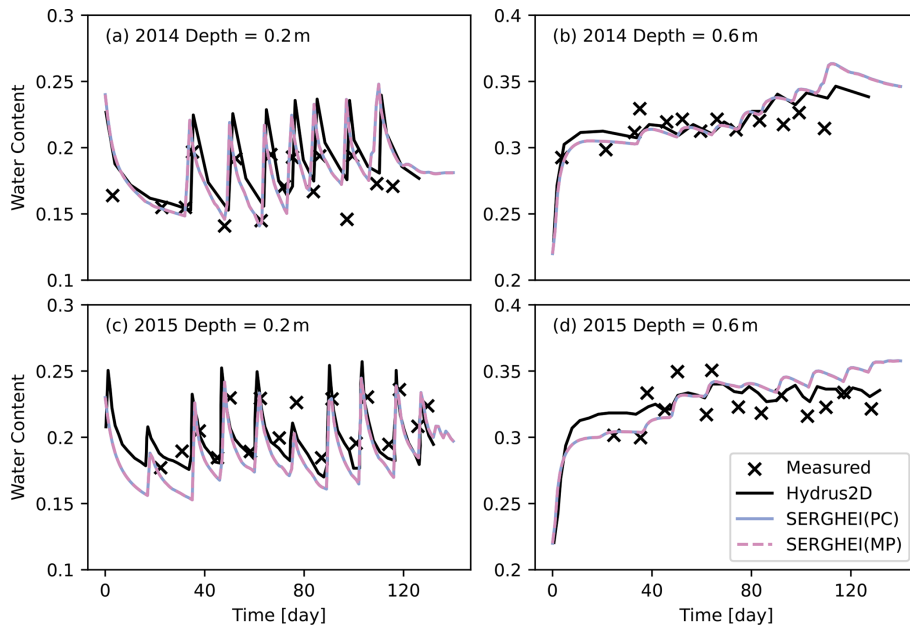


**Figure 12.** SERGHEI-RE simulation results (water content at 0.2 and 0.6 m beneath the irrigation dripper) of the crop irrigation problem against field measurements and Hydrus2D results.

This way, the need for varying domain sizes regarding scaling tests on different computational platforms can be accomplished. All other model inputs, such as the soil properties and the initial and boundary conditions, are kept the same as in Sect. 4.4. We demonstrate the scaling test results on three computational domains: a small domain with 1.2 million grid cells (10 rows in the  $y$  direction), a medium domain

with 15.36 million grid cells (128 rows), and a large domain with 120 million grid cells (1000 rows).

### 5.1 Small domain with 1.2 million cells

For the small domain test case, SERGHEI-RE is run with both the PC and MP schemes on two computational systems: (i) a Dell Precision 5820 desktop workstation equipped

with an Intel Xeon W-2265 CPU (3.5 GHz, 12 cores, 24 threads) and an Nvidia RTX A5000 GPU (24 GB memory, 768 GB s<sup>-1</sup> bandwidth, 8192 CUDA cores) and (ii) a small cluster at the high-performance computing center of Tongji University (named TJ HPC hereafter), where each CPU node is equipped with an Intel Xeon Max 9468 processor (3.5 GHz, 48 cores, 96 threads), and each GPU node is equipped with an Nvidia L40 GPU (48 GB memory, 864 GB s<sup>-1</sup> bandwidth, 18176 CUDA cores). For both systems, shared memory parallelization (OpenMP) is tested on a single CPU using a variable number of threads. On the TJ HPC cluster, an additional scenario is tested, where the computation task is split into four MPI processes on four nodes. Each node uses 1 to 64 OpenMP threads, beyond which the maximum allowed computational resources on the TJ HPC cluster are met. GPU tests are completed on single A5000 and L40 GPUs. Thus, systematic multi-CPU or multi-GPU parallelization tests are not performed herein – they are reserved for the medium and the large domains. For this test, the simulation length is set to 2 h with  $\Delta t_{\max} = 180$  s.

Figure 13 shows the simulation time and the speedup for different parallel configurations. It can be seen that on the desktop CPU the scaling is nearly ideal up to 12 threads. With 16 threads, the scaling begins to deteriorate. On the TJ HPC cluster, the speedup gradually deviates from linear beyond 16 threads but keeps increasing even at full capacity (96 threads). For the four-node scenario, the simulation scales well from 16 to 192 threads and then deteriorates at 256 threads. As expected, with the same  $\Delta t_{\max}$ , the MP scheme is computationally more expensive than the PC scheme, but the speedups are similar. This demonstrates, with the same amount of total threads, that splitting the work into multiple nodes effectively improves scaling. With a single GPU, the simulation time is dramatically reduced. The speedups are 89.4 and 269.7 relative to a single CPU thread for the A5000 and L40 GPUs, respectively. If compared to 96 threads of TJ HPC, the speedups are 1.7 and 6.1, respectively. This indicates that even on desktop workstations, GPU-based SERGHEI-RE significantly enhances the computational efficiency compared to traditional CPU-based Richards solvers, making it a promising tool for large-scale variably saturated subsurface flow simulations.

## 5.2 Medium domain with 15.36 million cells

In this test case, SERGHEI-RE is deployed on the LISE HPC system of the German National High Performance Computing (NHR) Alliance at Zuse Institute Berlin, Germany. Each computation node of LISE is equipped with two units of Intel Xeon Platinum 9242 processors (2.30 GHz, 48 cores, 96 threads). The simulation length is set to 6 h with  $\Delta t_{\max} = 180$  s. The simulation time and the speedup (with the PC scheme) for different parallel configurations is shown in Fig. 14. The speedup curve is approximately 73%–84% more efficient compared to ideal linear scaling from 2 to 128

nodes with the observed maximum efficiency of 84.4% at 32 nodes. Increasing deterioration in scaling emerges beyond 128 nodes with 256 and 512 nodes being 51% and 27% more efficient, respectively. These results indicate that SERGHEI-RE achieves good scaling performance up to 128 nodes for the medium domain on CPU-based HPC systems, successfully demonstrating its performance portability. Table 5 shows that the PCG solver of Kokkos Kernels takes more than 80% of the total simulation time from 1 to 128 nodes and decreases with more nodes being used. Furthermore, the speedup of the linear solver is slightly higher than the overall speedup of the simulation, suggesting that the scaling performance is mainly attributed to the PCG solver. A similar finding is reported in Li et al. (2024).

## 5.3 Large domain with 120 million cells

For testing the large domain, SERGHEI-RE is deployed on the JUWELS (cluster and booster) system at the Jülich Supercomputing Center. Each JUWELS cluster GPU node contains four Nvidia Tesla V100 GPU cards (32 GB memory, 900 GB s<sup>-1</sup> bandwidth). Each JUWELS booster node contains four Nvidia A100 Tensor Core GPU cards (80 GB memory, 1935 GB s<sup>-1</sup> bandwidth). The simulation length is set to 6 h with  $\Delta t_{\max} = 180$  s. Figure 15 shows the simulation time and the speedup on the JUWELS cluster and the JUWELS booster nodes. It can be seen from Fig. 15 that at up to 64 nodes the speedup curves are approximately linear on both V100 and A100 GPUs and for both PC and MP schemes. Superlinear speedup is observed from 2 to 32 GPU nodes. Beyond 64 GPU nodes, the scaling starts to deteriorate with the PC scheme showing stronger deterioration than the MP scheme. This is because the linear system solver takes a greater portion of the total simulation time for the iterative MP scheme, and the linear solver scales well (see Li et al., 2024, and Table 5 for further discussion). Figure 15 clearly shows that the MP scheme is substantially more expensive than the PC scheme, although they use the same  $\Delta t_{\max}$ . Nonetheless, the scaling behavior is very similar with fewer than 64 nodes, which is a clear indication that the number of linearization steps in the MP scheme is responsible for the computational overhead.

Table 5 illustrates that the linear system solver (i.e., the PCG solver of Kokkos Kernels) takes more than 94% of the total simulation time for 1 to 32 GPU nodes. Similar to LISE, with more nodes used, the proportion of solver time decreases on the JUWELS booster. Furthermore, the speedup of the linear solver is higher than the overall speedup as more nodes are used. Again, this means that the good scaling performance is mainly attributed to the good scaling of the Kokkos Kernels solver. At 160 nodes, the linear solver only takes 61.7% of the simulation time. Although the solver speedup exceeds 120, the overall speedup is only 78.93. Detailed examination (not shown) reveals that at 160 nodes the MPI exchange time is comparable with the linear solver time,

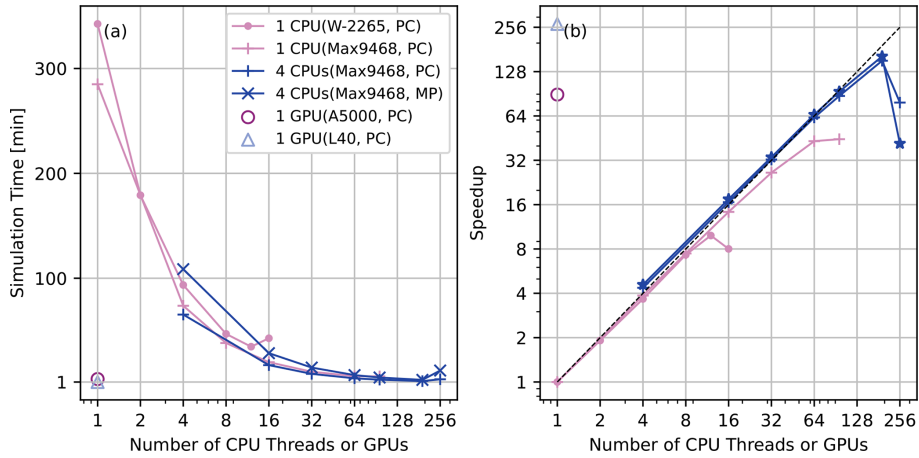


**Figure 13.** (a) SERGHEI-RE simulation time and (b) speedup on a desktop workstation and on the TJ HPC cluster. The test problem has 1.2 million grid cells. Note that the horizontal axis is the number of CPU threads (i.e., the number of CPUs times the number of threads used per CPU) or the number of GPUs.

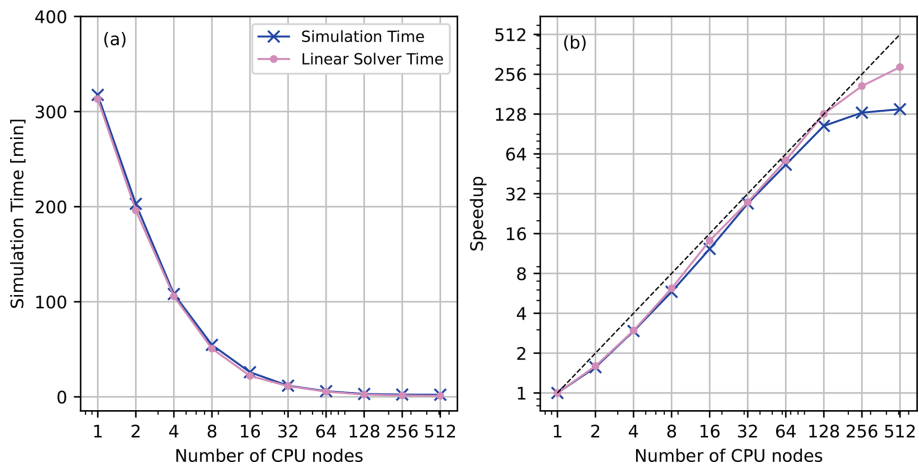


**Figure 14.** SERGHEI-RE simulation time and speedup on the LISE HPC with Intel Xeon Platinum 9242 CPUs. The test problem has 15.36 million grid cells.

indicating that (given the dimension of this test problem), too many GPUs are used, which squeezes the dimension of the subdomains, resulting in suboptimal scaling performance (with 160 nodes, each subdomain contains  $25 \times 50 \times 150$  grid cells in the  $x$ ,  $y$ , and  $z$  directions, respectively). Table 5 also provides the ratio of simulation times between the MP and PC schemes on the JUWELS booster, which is always greater than one. This result is consistent with Fig. 15, illustrating that given the same  $\Delta t_{\max}$  the MP scheme is computationally more expensive than the PC scheme regardless of the parallelization configurations. Overall, Table 5 demonstrates similar scaling performance (i.e., near-linear to superlinear speedup, good scaling of the linear solver) on both multi-CPU and multi-GPU HPC systems, highlighting the performance portability of the SERGHEI-RE model.

## 6 Conclusions

In this paper, we present SERGHEI-RE, the variably saturated subsurface flow simulation module of SERGHEI. SERGHEI-RE provides both an iterative and a non-iterative numerical scheme for subsurface flow simulation. This enhances model flexibility under various simulation conditions that could make the numerical solution to the 3D Richards equation challenging. By testing SERGHEI-RE on six benchmark problems, ranging from simple infiltration and drainage to realistic hydrological, geotechnical, and agricultural applications, we show that SERGHEI-RE produces satisfactory agreements with experimental measurements, field observations, and/or simulation results with other software. We demonstrate that the numerical scheme of SERGHEI-RE is accurate, robust, and versatile.

**Table 5.** Speedup comparison for the entire simulation, the linear solver (PCG), and the proportion of the linear solver on the runtime for the PC scheme scenarios on the LISE HPC (Fig. 14) and JUWELS booster HPC clusters (Fig. 15). Efficiency is determined as the quotient of speedup and node count. The last row shows the ratio of simulation times between the MP and PC schemes on the JUWELS booster.

LISE nodes	1	2	4	8	16	32	64	128	256	512
Speedup	1.000	1.565	2.936	5.811	12.257	27.005	53.062	104.174	131.212	139.256
Speedup (PCG)	1.000	1.597	2.961	6.168	14.159	27.627	57.286	128.429	208.469	289.725
Efficiency	100.0 %	78.2 %	73.4 %	72.6 %	76.6 %	84.4 %	82.9 %	81.4 %	51.3 %	27.2 %
Efficiency (PCG)	100.0 %	79.8 %	74.0 %	77.1 %	88.5 %	86.3 %	89.5 %	100.3 %	81.4 %	56.6 %
Proportion of runtime	98.6 %	96.6 %	97.8 %	92.9 %	85.4 %	96.4 %	91.3 %	80.0 %	62.1 %	47.4 %
JUWELS A100 nodes	1	2	4	8	16	32	64	160	320	–
Speedup	1.000	2.020	4.141	8.484	16.997	32.292	57.550	78.93	74.10	–
Speedup (PCG)	1.000	2.022	4.159	8.574	17.446	33.928	63.979	127.67	202.06	–
Efficiency	100.0 %	101.0 %	103.5 %	106.1 %	106.2 %	100.9 %	89.9 %	49.3 %	23.2 %	–
Efficiency (PCG)	100.0 %	101.1 %	104.0 %	107.2 %	109.0 %	106.0 %	100.0 %	79.8 %	63.1 %	–
Proportion of runtime	99.7 %	99.6 %	99.3 %	98.7 %	97.2 %	94.9 %	89.7 %	61.7 %	36.6 %	–
Sim. time (MP/PC)	3.212	3.270	3.237	3.263	3.238	3.244	3.050	2.312	1.793	–

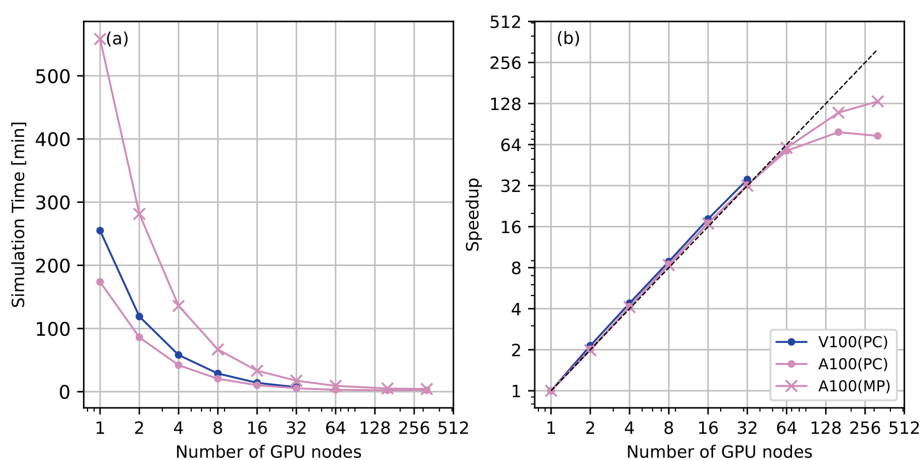


**Figure 15.** (a) SERGHEI-RE simulation time and (b) speedup on Nvidia V100 and A100 GPUs equipped on the JUWELS HPC cluster. The test problem has 120 million grid cells.

SERGHEI-RE is developed within the SERGHEI framework, meaning that it is equipped with the Kokkos programming model to achieve performance-portable parallelization on various computational devices. We show that SERGHEI-RE scales well on personal desktop workstations, and on multi-CPU and multi-GPU supercomputers, thereby demonstrating its performance-portable scalability that is critical for subsurface flow models aimed towards environmental applications, while simultaneously fully aligning with the evolving computational advancements into the exascale era. SERGHEI-RE shows very good scalability with both the predictor-corrector (PC) and the well-established fully implicit modified Picard (MP) schemes. The MP scheme typically allows for a greater time step size to enhance computational efficiency, but it is computationally more expensive per time step as it is iterative.

Variably saturated subsurface flow simulation is at the core of hydrological simulations. However, realistic engineering applications also require additional modeling capabilities such as surface–subsurface flow exchange, reactive transport, and vegetation dynamics. As shown in Fig. 1, these (and more) functions are being developed and tested. Additional modules are expected to be released in the near future, extending the applicability of SERGHEI to the broad range of computational hydrology.

*Code and data availability.* SERGHEI is available through GitLab, at <https://gitlab.com/serghei-model/serghei> (last access: 4 August 2024), under the 3-Clause BSD License. The SERGHEI-RE source code is tagged as SERGHEI v2.0. A static version of SERGHEI-RE (SERGHEI v2.0) is archived on Zenodo, with DOI <https://doi.org/10.5281/zenodo.13166466> (Caviedes-Voullième et al., 2024). Developer and user guides are available

on the wiki page of the SERGHEI project. The following tools and packages are a prerequisite for SERGHEI-RE: GCC (other C++ compilers have not been tested), OpenMPI (other MPI implementations have not been thoroughly tested), CMake, Kokkos, KokkosKernels, and PnetCDF.

The input files of the test cases reported in this paper are available in the “serghei-tests” repository on GitLab (<https://gitlab.com/serghei-model/serghei-tests/subsurface/analytical> and <https://gitlab.com/serghei-model/serghei-tests/subsurface/experimental>, last access: 4 August 2024). A static version of the tests is archived on Zenodo, with DOI <https://doi.org/10.5281/zenodo.13282882> (Li, 2024).

*Author contributions.* ZL contributed to conceptualization, methodology, software, formal analysis, and writing (original draft). GR contributed to formal analysis and writing (original draft). NZ contributed to software, formal analysis and writing (review and editing). ZZ contributed to formal analysis and writing (review and editing). IOX contributed to formal analysis and writing (review and editing). DCV contributed to conceptualization, software, and writing (review and editing).

*Competing interests.* The contact author has declared that none of the authors has any competing interests.

*Disclaimer.* Publisher’s note: Copernicus Publications remains neutral with regard to jurisdictional claims made in the text, published maps, institutional affiliations, or any other geographical representation in this paper. While Copernicus Publications makes every effort to include appropriate place names, the final responsibility lies with the authors.

*Acknowledgements.* This study is supported by the National Natural Science Foundation of China (NSFC grant no. 42307078), the National Key R&D Program of China (2022YFC3803001), and the Fundamental Research Funds for the Central Universities (China). Ilhan Özgen-Xian and Gregor Rickert are funded by the Tenure-Track Programme of the German Ministry of Education and Research. This work used HPC resources provided by the Center for Scientific Computing at Tongji University, China, and the German National High Performance Computing (NHR) Alliance at Zuse Institute Berlin (ZIB), Germany. The authors gratefully acknowledge the Earth System Modelling (ESM) project for supporting this work by providing computing time on the ESM partition of the JUWELS supercomputer at the Jülich Supercomputing Centre (JSC) through the compute time project “Runoff Generation and Surface Hydrodynamics across Scales with the SERGHEI model” (RUGSHAS) (project nos. 22686 and 29000).

*Financial support.* The manuscript registration fee will be covered by the National Natural Science Foundation of China (NSFC grant no. 42307078), the National Key R&D Program of China (2022YFC3803001), and the Fundamental Research Funds for the Central Universities (China).

*Review statement.* This paper was edited by Charles Onyutha and reviewed by two anonymous referees.

## References

- Abeele, W. V.: Hydraulic testing of crushed Bandelier Tuff, Tech. rep., U.S. Department of Energy, <https://www.osti.gov/biblio/60528> (last access: 30 January 2025), 1984.
- Bassetto, S., Cancès, C., Enchéry, G., and Tran, Q.-H.: On several numerical strategies to solve Richards’ equation in heterogeneous media with finite volumes, *Comput. Geosci.*, 26, 1297–1322, <https://doi.org/10.1007/s10596-022-10150-w>, 2022.
- Beegum, S., Šimůnek, J., Szymkiewicz, A., Sudheer, K., and Nambi, I. M.: Updating the Coupling Algorithm between HYDRUS and MODFLOW in the HYDRUS Package for MODFLOW, *Vadose Zone J.*, 17, 1–8, <https://doi.org/10.2136/vzj2018.02.0034>, 2018.
- Brandhorst, N., Erdal, D., and Neuweiler, I.: Coupling saturated and unsaturated flow: comparing the iterative and the non-iterative approach, *Hydrol. Earth Syst. Sci.*, 25, 4041–4059, <https://doi.org/10.5194/hess-25-4041-2021>, 2021.
- Caviedes-Voullième, D., García-Navarro, P., and Murillo, J.: Verification, conservation, stability and efficiency of a finite volume method for the 1D Richards equation, *J. Hydrol.*, 480, 69–84, <https://doi.org/10.1016/j.jhydrol.2012.12.008>, 2013.
- Caviedes-Voullième, D., Morales-Hernández, M., Norman, M. R., and Özgen-Xian, I.: SERGHEI (SERGHEI-SWE) v1.0: a performance-portable high-performance parallel-computing shallow-water solver for hydrology and environmental hydraulics, *Geosci. Model Dev.*, 16, 977–1008, <https://doi.org/10.5194/gmd-16-977-2023>, 2023.
- Caviedes-Voullième, D., Morales-Hernández, M., and Özgen Xian, I.: SERGHEI (2.0), Zenodo [code], <https://doi.org/10.5281/zenodo.13166466>, 2024.
- Celia, M. A., Bouloutas, E. T., and Zarba, R. L.: A general mass-conservative numerical solution for the unsaturated flow equation, *Water Resour. Res.*, 26, 1483–1496, <https://doi.org/10.1029/WR026i007p01483>, 1990.
- Chang, C., Deringer, V. L., Katti, K. S., Van Speybroeck, V., and Wolverson, C. M.: Simulations in the era of exascale computing, *Nat. Rev. Mater.*, 8, 309–313, <https://doi.org/10.1038/s41578-023-00540-6>, 2023.
- Chávez-Negrete, C., Domínguez-Mota, F., and Santana-Quinteros, D.: Numerical solution of Richards equation of water flow by generalized finite differences, *Comput. Geotech.*, 101, 168–175, <https://doi.org/10.1016/j.compgeo.2018.05.003>, 2018.
- Condon, L. E., Markovich, K. H., Kelleher, C. A., McDonnell, J. J., Ferguson, G., and McIntosh, J. C.: Where is the bottom of the watershed?, *Water Resour. Res.*, 56, e2019WR026010, <https://doi.org/10.1029/2019WR026010>, 2020.
- Coon, E. T., Svyatskiy, D., Jan, A., Kikinon, E., Berndt, M., Atchley, A. L., Harp, D. R., Manzini, G., Shelef, E., Lipnikov, K., Garimella, R., Xu, C., Moulton, J. D., Karra, S., Painter, S. L., Jafarov, E., and Molins, S.: Advanced Terrestrial Simulator (ATS), USDOE Office of Science (SC) [code], <https://doi.org/10.11578/dc.20190911.1>, 2019.
- D’Haese, C. M. F., Putti, M., Paniconi, C., and Verhoest, N. E. C.: Assessment of adaptive and heuristic time stepping for vari-

- ably saturated flow, *Int. J. Numer. Meth. Fl.*, 53, 1173–1193, <https://doi.org/10.1002/fld.1369>, 2007.
- El-Kadi, A. I. and Ling, G.: The Courant and Peclet Number criteria for the numerical solution of the Richards Equation, *Water Resour. Res.*, 29, 3485–3494, <https://doi.org/10.1029/93WR00929>, 1993.
- Farthing, M. W. and Ogden, F. L.: Numerical Solution of Richards' Equation: A Review of Advances and Challenges, *Soil Sci. Soc. Am. J.*, 81, 1257–1269, <https://doi.org/10.2136/sssaj2017.02.0058>, 2017.
- Forsyth, P., Wu, Y., and Pruess, K.: Robust numerical methods for saturated-unsaturated flow with dry initial conditions in heterogeneous media, *Adv. Water Resour.*, 18, 25–38, [https://doi.org/10.1016/0309-1708\(95\)00020-J](https://doi.org/10.1016/0309-1708(95)00020-J), 1995.
- Hammond, G. E., Lichtner, P. C., and Mills, R. T.: Evaluating the performance of parallel subsurface simulators: An illustrative example with PFLOTRAN, *Water Resour. Res.*, 50, 208–228, <https://doi.org/10.1002/2012WR013483>, 2014.
- He, Q., Li, S., Kang, S., Yang, H., and Qin, S.: Simulation of water balance in a maize field under film-mulching drip irrigation, *Agr. Water Manage.*, 210, 252–260, <https://doi.org/10.1016/j.agwat.2018.08.005>, 2018.
- Hokkanen, J., Kollet, S., Kraus, J., Herten, A., Hrywniak, M., and Pleiter, D.: Leveraging HPC accelerator architectures with modern techniques — hydrologic modeling on GPUs with ParFlow, *Comput. Geosci.*, 25, 1579–1590, <https://doi.org/10.1007/s10596-021-10051-4>, 2021.
- Hou, J., Pan, Z., Tong, Y., Li, X., Zheng, J., and Kang, Y.: High-efficiency and high-resolution numerical modeling for two-dimensional infiltration processes, accelerated by a graphics processing unit, *Hydrogeol. J.*, 30, 637–651, <https://doi.org/10.1007/s10040-021-02444-7>, 2022.
- Kirkland, M. R., Hills, R. G., and Wierenga, P. J.: Algorithms for solving Richards' equation for variably saturated soils, *Water Resour. Res.*, 28, 2049–2058, <https://doi.org/10.1029/92WR00802>, 1992.
- Kollet, S. J. and Maxwell, R. M.: Integrated surface–groundwater flow modeling: A free-surface overland flow boundary condition in a parallel groundwater flow model, *Adv. Water Resour.*, 29, 945–958, <https://doi.org/10.1016/j.advwatres.2005.08.006>, 2006.
- Kuffour, B. N. O., Engdahl, N. B., Woodward, C. S., Condon, L. E., Kollet, S., and Maxwell, R. M.: Simulating coupled surface–subsurface flows with ParFlow v3.5.0: capabilities, applications, and ongoing development of an open-source, massively parallel, integrated hydrologic model, *Geosci. Model Dev.*, 13, 1373–1397, <https://doi.org/10.5194/gmd-13-1373-2020>, 2020.
- Lai, W. and Ogden, F. L.: A mass-conservative finite volume predictor–corrector solution of the 1D Richards' equation, *J. Hydrol.*, 523, 119–127, <https://doi.org/10.1016/j.jhydrol.2015.01.053>, 2015.
- Li, Z.: Test cases for SERGHEI v2.0 (SERGHEI-RE), Zenodo [data set], <https://doi.org/10.5281/zenodo.13282882>, 2024.
- Li, Z., Özgen Xian, I., and Maina, F. Z.: A mass-conservative predictor-corrector solution to the 1D Richards equation with adaptive time control, *J. Hydrol.*, 592, 125809, <https://doi.org/10.1016/j.jhydrol.2020.125809>, 2021.
- Li, Z., Hodges, B. R., and Shen, X.: Modeling hypersalinity caused by evaporation and surface–subsurface exchange in a coastal marsh, *J. Hydrol.*, 618, 129268, <https://doi.org/10.1016/j.jhydrol.2023.129268>, 2023.
- Li, Z., Caviedes-Voullième, D., Özgen Xian, I., Jiang, S., and Zheng, N.: A comparison of numerical schemes for the GPU-accelerated simulation of variably-saturated groundwater flow, *Environ. Modell. Softw.*, 171, 105900, <https://doi.org/10.1016/j.envsoft.2023.105900>, 2024.
- Mao, W., Zhu, Y., Ye, M., Zhang, X., Wu, J., and Yang, J.: A new quasi-3-D model with a dual iterative coupling scheme for simulating unsaturated-saturated water flow and solute transport at a regional scale, *J. Hydrol.*, 602, 126780, <https://doi.org/10.1016/j.jhydrol.2021.126780>, 2021.
- Maxwell, R. M.: A terrain-following grid transform and preconditioner for parallel, large-scale, integrated hydrologic modeling, *Adv. Water Resour.*, 53, 109–117, <https://doi.org/10.1016/j.advwatres.2012.10.001>, 2013.
- Morway, E. D., Niswonger, R. G., Langevin, C. D., Bailey, R. T., and Healy, R. W.: Modeling Variably Saturated Subsurface Solute Transport with MODFLOW-UZF and MT3DMS, *Groundwater*, 51, 237–251, <https://doi.org/10.1111/j.1745-6584.2012.00971.x>, 2013.
- Mualem, Y.: A new model for predicting the hydraulic conductivity of unsaturated porous media, *Water Resour. Res.*, 12, 513–522, <https://doi.org/10.1029/WR012i003p00513>, 1976.
- Orgogozo, L., Renon, N., Soulaïne, C., Hénon, F., Tomer, S., Labat, D., Pokrovsky, O., Sekhar, M., Ababou, R., and Quintard, M.: An open source massively parallel solver for Richards equation: mechanistic modelling of water fluxes at the watershed scale, *Comput. Phys. Commun.*, 185, 3358–3371, <https://doi.org/10.1016/j.cpc.2014.08.004>, 2014.
- Özgen-Xian, I., Molins, S., Johnson, R. M., Xu, Z., Dwivedi, D., Loritz, R., Mital, U., Ulrich, C., Yan, Q., and Steefel, C. I.: Understanding the hydrological response of a headwater-dominated catchment by analysis of distributed surface–subsurface interactions, *Sci. Rep.*, 13, 4669, <https://doi.org/10.1038/s41598-023-31925-w>, 2023.
- Paniconi, C. and Putti, M.: A comparison of Picard and Newton iteration in the numerical solution of multidimensional variably saturated flow problems, *Water Resour. Res.*, 30, 3357–3374, <https://doi.org/10.1029/94WR02046>, 1994.
- Paniconi, C. and Putti, M.: Physically based modeling in catchment hydrology at 50: Survey and outlook, *Water Resour. Res.*, 51, 7090–7129, <https://doi.org/10.1002/2015WR017780>, 2015.
- Phoon, K., Tan, T., and Chong, P.: Numerical simulation of Richards equation in partially saturated porous media: under-relaxation and mass balance, *Geotech. Geol. Eng.*, 25, 525–541, <https://doi.org/10.1007/s10706-007-9126-7>, 2007.
- Richards, L. A.: Capillary conduction of liquids through porous mediums, *Physics*, 1, 318–333, 1931.
- Richardson, L. F.: *Weather Prediction by Numerical Process*, Cambridge University Press, Cambridge, UK, <https://doi.org/10.1017/CBO9780511618291>, 1922.
- Shen, C. and Phanikumar, M. S.: A process-based, distributed hydrologic model based on a large-scale method for surface–subsurface coupling, *Adv. Water Resour.*, 33, 1524–1541, <https://doi.org/10.1016/j.advwatres.2010.09.002>, 2010.
- Šimůnek, J., Šejna, M., Saito, H., Sakai, M., and van Genuchten, M. T.: *The HYDRUS-1D Software Package for Simulating the One-Dimensional Movement of Water, Heat, and Multiple So-*

- lutes in Variably-Saturated Media v4.17, University of California Riverside, Riverside, California, [https://www.pc-progress.com/Downloads/Pgm\\_hydrus1D/HYDRUS1D-4.17.pdf](https://www.pc-progress.com/Downloads/Pgm_hydrus1D/HYDRUS1D-4.17.pdf) (last access: 4 August 2024), 2013.
- Šimůnek, J., van Genuchten, M. T., and Šejna, M.: Recent Developments and Applications of the HYDRUS Computer Software Packages, *Vadose Zone J.*, 15, 1–15, <https://doi.org/10.2136/vzj2016.04.0033>, 2016.
- Trott, C. R., Lebrun-Grandié, D., Arndt, D., Ciesko, J., Dang, V., Ellingwood, N., Gayatri, R., Harvey, E., Hollman, D. S., Ibanez, D., Liber, N., Madsen, J., Miles, J., Poliakoff, D., Powell, A., Rajamanickam, S., Simberg, M., Sunderland, D., Turcksin, B., and Wilke, J.: Kokkos 3: Programming Model Extensions for the Exascale Era, *IEEE T. Parallel Distr.*, 33, 805–817, <https://doi.org/10.1109/TPDS.2021.3097283>, 2022.
- van Genuchten, M.: A closed-form equation for predicting the hydraulic conductivity of unsaturated soils, *Soil Sci. Soc. Am. J.*, 44, 892–898, <https://doi.org/10.2136/sssaj1980.03615995004400050002x>, 1980.
- van Lier, Q. J. and Pinheiro, E. A. R.: An alert regarding a common misinterpretation of the van Genuchten  $\alpha$  parameter, *Rev. Bras. Ciênc. Solo*, 42, e0170343, <https://doi.org/10.1590/18069657rbc20170343>, 2018.
- Vogel, T.: Effect of the shape of the soil hydraulic functions near saturation on variably-saturated flow predictions, *Adv. Water Resour.*, 24, 133–144, [https://doi.org/10.1016/S0309-1708\(00\)00037-3](https://doi.org/10.1016/S0309-1708(00)00037-3), 2001.
- Warrick, A. W., Lomen, D. O., and Yates, S. R.: A Generalized Solution to Infiltration, *Soil Sci. Soc. Am. J.*, 49, 34–38, <https://doi.org/10.2136/sssaj1985.03615995004900010006x>, 1985.
- Zha, Y., Tso, M. C.-H., Shi, L., and Yang, J.: Comparison of Noniterative Algorithms Based on Different Forms of Richards' Equation, *Environ. Model. Assess.*, 21, 357–370, <https://doi.org/10.1007/s10666-015-9467-1>, 2016.
- Zha, Y., Yang, J., Yin, L., Zhang, Y., Zeng, W., and Shi, L.: A modified Picard iteration scheme for overcoming numerical difficulties of simulating infiltration into dry soil, *J. Hydrol.*, 551, 56–69, <https://doi.org/10.1016/j.jhydrol.2017.05.053>, 2017.
- Zha, Y., Yang, J., Zeng, J., Tso, C. M., Zeng, W., and Shi, L.: Review of numerical solution of Richardson–Richards equation for variably saturated flow in soils, *WIREs Water*, 6, e1364, <https://doi.org/10.1002/wat2.1364>, 2019.
- Zhang, Z., Wang, W., Gong, C., Jim Yeh, T.-C., Duan, L., and Wang, Z.: Finite analytic method: Analysis of one-dimensional vertical unsaturated flow in layered soils, *J. Hydrol.*, 597, 125716, <https://doi.org/10.1016/j.jhydrol.2020.125716>, 2021.